

# Electron correlations and bond-length fluctuations in copper oxides: from Zhang–Rice singlets to correlation bags

L. Hozoi,<sup>1</sup> S. Nishimoto,<sup>2</sup> and A. Yamasaki<sup>1</sup>

<sup>1</sup>Max-Planck-Institut für Festkörperforschung, Heisenbergstrasse 1, 70569 Stuttgart, Germany

<sup>2</sup>Institut für Theoretische Physik, Universität Göttingen,  
Friedrich-Hund-Platz 1, 37077 Göttingen, Germany

(Dated: November 16, 2018)

We perform first principles, multiconfiguration calculations on clusters including several  $\text{CuO}_6$  octahedra and study the ground-state electron distribution and electron–lattice couplings when holes are added to the undoped  $d^9 p^6$  configuration. We find that the so-called Zhang–Rice state on a single  $\text{CuO}_4$  plaquette is nearly degenerate with a state whose leading configuration is of the form  $\text{Cu } d^9 - \text{O } p^5 - \text{Cu } d^9$ . A strong coupling between the electronic and nuclear motion gives rise to large inter-site charge transfer effects for half-breathing displacements of the oxygen ions. Under the assumption of charge segregation into alternating hole-free and hole-rich stripes of Goodenough [1, 2], our results seem to support the vibronic mechanism and the traveling charge-density wave model from Refs.[1, 2] for the superconductivity in copper oxides.

## I. INTRODUCTION

It is widely believed that the lattice degrees of freedom should play some role in the high- $T_c$  superconductivity in doped copper oxides. In a recent series of articles, see for example [1, 2, 3], J. B. Goodenough and coworkers predict for these systems the existence of strong lattice instabilities associated with two distinguishable (equilibrium) Cu–O bond lengths and suggest that long range “ordering” of bond-length fluctuations would stabilize some kind of traveling charge-density wave (CDW) in the superconducting state. Goodenough *et al.* propose a model where the hole–hole Coulomb repulsion and relatively strong antiferromagnetic (AFM)  $d^9 - d^9$  couplings give rise at  $x = 1/6$  doping and low temperatures to a configuration with alternating, 1/3-doped and hole-free, Cu–O–... stripes. Within the 1/3-doped Cu–O–... rows the holes occupy Cu–O–Cu bonding orbitals. The superconductivity is associated in Refs.[1, 2, 3] with itinerant heavy vibrons that originate from the coupling between some particular (dynamic) ordering of these Cu–O–Cu “hole bags” and in-plane phonons.

The present paper is an attempt towards a better understanding of the nature of the local electron–electron and electron–lattice interactions in copper oxides. We employ *ab initio* methods from traditional quantum chemistry. Our calculations are performed on finite clusters including several  $\text{CuO}_6$  octahedra. We pay special attention to the situation where one hole is added to the undoped, formally  $\text{Cu } d^9 \text{ O } p^6$ , configuration. Results from a square 5-octahedra cluster indicate that the so-called Zhang–Rice (ZR) singlet on a  $\text{CuO}_4$  plaquette [4] may become “unstable” with respect to a lower symmetry oxygen-hole state with a  $\text{Cu } d^9 - \text{O } p^5 - \text{Cu } d^9$  leading configuration. This is just the 1-hole Cu–O–Cu correlation bag of Goodenough [1]. We further investigate local interactions within a 1-hole, 4-octahedra linear cluster. We find evidence for strongly anharmonic, Jahn–Teller (JT) type effects for certain Cu–O bond distortions. The

oxygen-atom vibrations are coupled with strong inter-site charge transfer (CT) effects. Our findings seem to support a mechanism of the type proposed by Goodenough *et al.* [1, 2, 3] for the high temperature superconductivity.

It was suggested in Ref. [2] that at  $x = 1/6$  doping 1-hole Cu–O–Cu units could cluster to form spin-paired 2-hole bags including four Cu centres. A hypothetical ordered configuration of such 2-hole bags is shown in Fig.1(a). In a Zhang–Rice picture, the 1/3-doped stripes can be represented as in Fig.1(b), for example. Our analysis is carried out on 1-hole clusters corresponding to a somewhat intermediate arrangement, as we shall discuss below.

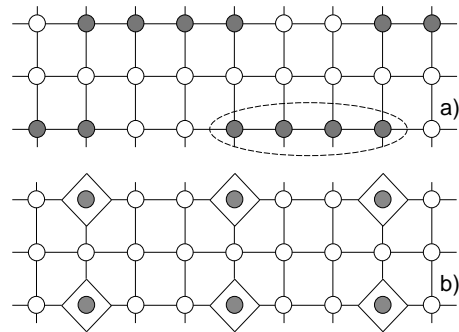


FIG. 1: (a) 2-(doped-)hole, 4-Cu correlation bags in the  $\text{CuO}$  plane at 1/6-doping as suggested by Goodenough [2], see text. Only the Cu sites are shown. A hole-free ( $d^9 p^6$ ) chain is drawn with open circles. (b) Hole-free and 1/3-doped stripes in a Zhang–Rice picture. The squares represent ZR singlets on  $\text{CuO}_4$  plaquettes. A relative shift between neighboring doped stripes should minimize the Coulomb repulsion. Intuitively, a 2-hole correlation bag forms by “clustering” of two ZR singlets.

## II. LOCAL CORRELATIONS IN THE CUO PLANE: $\text{CuO}_4$ ZHANG-RICE SINGLETS VERSUS $\text{Cu } d^9\text{-O } p^5\text{-Cu } d^9$ CONFIGURATIONS

First, we perform electronic structure calculations on a square cluster including a central  $\text{CuO}_6$  octahedron and the four adjacent in-plane octahedra. This  $[\text{Cu}_5\text{O}_{26}]$  cluster is embedded in a matrix of point charges that reproduce the Madelung potential associated to the undoped  $\text{La}_2\text{CuO}_4$  crystal. The nearest neighbor cations are represented by effective ion potentials. We use the tetragonal crystal structure of  $\text{La}_{1.85}\text{Sr}_{0.15}\text{CuO}_4$  as reported by Cava *et al.* [5], with in-plane Cu–O distances of 1.89 Å.

We rely on an *ab initio*, wave-function-based multi-configuration (MC) approach [6]. Our starting point is a Hartree–Fock self-consistent-field (SCF) calculation for a closed-shell  $\text{Cu } d^{10} \text{O } p^6$  configuration of the  $[\text{Cu}_5\text{O}_{26}]$  cluster. We remove then six electrons. We construct thus a multi-determinant (or multi-configuration) wave-function where “on top” of a number of closed electron shells six electrons/holes are distributed in all the possible ways over six orbitals. Such a configurational space is referred to as a complete active space (CAS) [6]. Those electrons and those orbitals defining the MC space are called active. Due to the relatively large size of the cluster we use effective core potentials (ECPs) for the Cu  $1s, 2s, 2p, 3s$  and the four bridging-oxygen ( $\text{O}_b^i$ , see Fig.2)  $1s$  core shells. The ECP basis sets of Huzinaga *et al.* [7] were applied for these ions, with the following contractions: Cu  $9s6p6d/2s2p3d$  and O  $5s6p1d/2s3p1d$ . For the other oxygens we applied the basis set of Widmark *et al.* [8] contracted to  $2s2p$ . All calculations were performed with the MOLCAS program package [9].

Unexpectedly, for an undistorted structure with identical Cu–O distances, the CAS SCF ground-state optimization converged to a broken-symmetry triplet state where the largest weight corresponds to a  $\text{Cu}_c d_{x^2-y^2}^1 - \text{O}_b^1 p_y^1 - \text{Cu}_{sq}^1 d_{x^2-y^2}^1$  configuration (see Fig.2(a)), although our 5-octahedra cluster has full  $D_{4h}$  symmetry [10]. The  $\text{O}_b^1 p_y$  and  $\text{Cu}_{sq}^1 d_{x^2-y^2}$  atomic orbitals form in this geometry bonding and antibonding combinations. Contributions from the  $\text{Cu}_c d_{x^2-y^2}$  and  $p_x/p_y$  orbitals on ligands adjacent to the  $\text{Cu}_{sq}^1$  cation to this pair of bonding and antibonding orbitals, while also present, are much smaller. Due to correlation, not only the bonding orbital is occupied but a partial charge transfer into the antibonding orbital occurs. The latter has an occupation number of 0.27, in comparison to 1.73 for the former. The formation of such a  $\text{Cu}_{sq} d_{x^2-y^2} - \text{O}_b^1 p_y$  bond favors antiferromagnetic  $d_{x^2-y^2} - d_{x^2-y^2}$  interactions over the other three bridging oxygens.

It turns out that the so-called ZR state, where the oxygen hole is equally distributed over four anions (Fig.2(b)), is approximately 80 meV above the broken-symmetry state with overall triplet spin multiplicity. Our data also indicate that it costs 44 meV to couple ferromagnetically those three  $\text{Cu}_{sq} d_{x^2-y^2}$  electrons to the  $\text{Cu}_c d_{x^2-y^2}$  (Fig.2(c)). Next, we determine the positions of

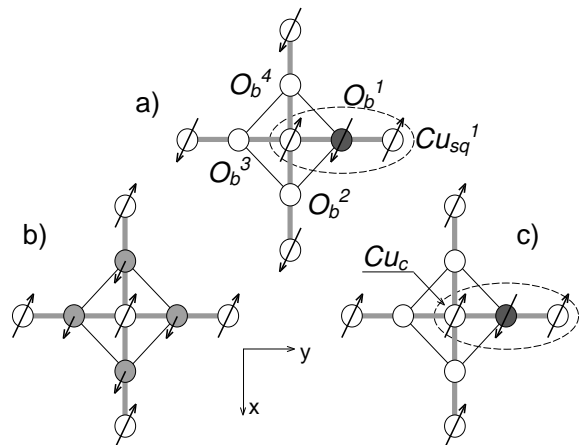


FIG. 2: (a) Leading configuration for the broken-symmetry, lowest-energy state in the geometry with identical Cu–O distances, see text. A  $\text{CuO}_4$  plaquette and four in-plane Cu neighbors are shown. (b) Schematic representation of the ZR state on our cluster. (c) Leading configuration for the lowest excited state in the undistorted structure. The  $d$ – $d$  couplings are ferromagnetic.

the bridging oxygens  $\text{O}_b^i$  that correspond to a minimum of the cluster total energy. According to our results this is the structure where the four  $\text{Cu}_c\text{-O}_b^i$  bonds are all about 5% shorter. For this arrangement, the ground state is a ZR like state with full  $D_{4h}$  symmetry. No broken-symmetry solution could be obtained for this geometry. Now, if we compare Fig.2(b) with Fig.2(c) (or Fig.2(a)) we can imagine the following scenario: starting from the minimum-energy structural configuration with shorter  $\text{Cu}_c\text{-O}_b^i$  bonds and a ZR electronic ground state, (half-)breathing displacements of the  $\text{O}_b$  oxygens may result in a broken-symmetry state where the leading configuration is of the form  $\text{Cu } d_{x^2-y^2}^1 - \text{O } p_y^1 - \text{Cu } d_{x^2-y^2}^1$  and the oxygen  $2p$  hole has the largest weight (*i.e.* is partially transferred, about 0.3 of an electron charge) onto a single anion. It is important to mention that the wave functions and the relative energies for the states discussed above remain largely unchanged when the active space is extended to include more ligand  $2p$  orbitals, such as the other linear combinations involving  $\text{O}_b p_y/p_x$  bridging orbitals.

It would be useful to determine how the cluster charge distribution changes for oxygen-atom distortions on an adjacent  $\text{CuO}_4$  plaquette. However, due to hardware limitations we could not employ sufficiently accurate basis sets for those oxygens beyond the nearest neighbors of the central Cu ion. To study such effects, the “cheapest” option is a 1-hole, 2-octahedra cluster. Calculations on this cluster reveal strong charge fluctuations between the two symmetric, minimum-energy geometrical configurations where the in-plane Cu–O distances on only one of the plaquettes are 5–6% shorter. For each of these distorted configurations, the doped hole has the largest weight on a single  $\text{O}_4$  plaquette and forms a ZR type sin-

plet with the Cu  $3d$  hole. In the undistorted geometry, the oxygen hole is mostly localized on the ligand bridging the two octahedra. The energy of the high-symmetry state is about 200 meV higher as compared to the ZR like configurations. The results indicate strong anharmonic effects, *i.e.* a one-dimensional double-well, when shifting the bridging oxygen along the  $y$  axis. This is analyzed in the next section.

For an *isolated*  $\text{Cu}_c\text{O}_6$  octahedron (or an isolated 5-octahedra square cluster) with no distortions, the simplest way to view the 1-doped-hole ground-state wave-function is as a superposition of the four broken-symmetry, degenerate  $\text{Cu}_c^{2+}-\text{O}^-$  solutions, see for example the discussion in [11]. Nevertheless, the calculations on the 2-octahedra cluster show that there is a finite probability for the ZR singlet to hop to an adjacent plaquette via such an intermediate broken-symmetry state with a dominant  $d^9-p^5-d^9$  configuration. (Meta)stable  $d^9-p^5-d^9$  configurations could actually be induced by longer range Coulomb interactions and AFM spin correlations in the doped plane. It seems then that the existence of 1-(doped-)hole Cu–O–Cu entities that could eventually cluster to form multi-hole correlation bags, as suggested by Goodenough [1, 2], is not an unrealistic hypothesis.

### III. 1-HOLE, 4-OCTAHEDRA LINEAR CLUSTERS: BOND-LENGTH FLUCTUATIONS AND INTER-SITE CHARGE TRANSFER

Inspired by the work of Goodenough *et al.* [1, 2, 3] we investigate local many-body effects and electron-lattice interactions within a 1-(doped-)hole, 4-octahedra [ $\text{Cu}_4\text{O}_{21}$ ] linear cluster. We apply  $C_{2v}$  symmetry restrictions, with  $xy$  and  $zy$  mirror planes (see Fig.3), and all-electron basis sets: Cu  $21s15p10d/5s4p3d$  [12], O  $14s9p4d/4s3p1d$  for the bridging  $\text{O}_b$  oxygens and O  $14s9p/4s3p$  for the other oxygens [8].

Starting from an undistorted structure with identical Cu–O distances, we perform a number of test calculations to identify the geometry that minimizes the cluster total energy. However, only the chain Cu and  $\text{O}_b$  ions are allowed to move, along the  $y$  axis. We do not modify the positions of the in-plane oxygens adjacent to the CuO chain,  $\text{O}_a^i$ , or the positions of the apical ligands. We employ a 5 electron / 5 orbital CAS, with five electrons being removed from the closed-shell Cu  $d^{10}$   $\text{O} p^6$  configuration. It is found that the lowest-energy geometry corresponds to a distorted configuration like that shown in Fig.3(b). The  $\text{O}_b^c$  atom is shifted to the left by 6% of the high-symmetry Cu–O bond length and the  $\text{O}_b^l$  atom is shifted by 6% to the right. For this geometry an oxygen  $2p$  hole/electron is bound to the  $\text{Cu}_l$   $d_{x^2-y^2}$  hole/electron into a ZR like singlet state. We give in Table I the composition of the bonding (B) and antibonding (AB) active (natural) orbitals [13] on the  $\text{Cu}_l\text{O}_4$  plaquette, their occupation numbers and the Mulliken populations (MPs)

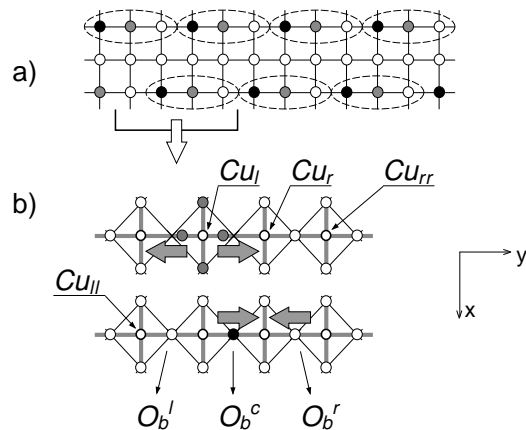


FIG. 3: (a) Possible charge-ordered configuration with 1-(doped-)hole, 3-Cu spin-singlet “correlation bags” along the 1/3-doped stripes, see text. Only the Cu sites are shown. A hole-free chain is drawn with open circles. (b) Four consecutive  $\text{CuO}_4$  plaquettes along the 1/3-doped chain. The CASCF calculations were carried out on such clusters. The O  $2p$  hole is represented with black or gray circles. For certain phases of the O-atom half-breathing vibrations the hole can hop along the chain. From left to right, the Cu and the bridging O atoms along the CuO chain are labeled as  $\text{Cu}_{ll}$ ,  $\text{Cu}_l$ ,  $\text{O}_b^l$ ,  $\text{O}_b^c$ ,  $\text{Cu}_r$ ,  $\text{O}_b^r$ , and  $\text{Cu}_{rr}$ .

for the relevant O  $2p$  and Cu  $3d$  atomic orbitals. The other three active orbitals have essentially  $\text{Cu}_{ll}$ ,  $\text{Cu}_r$  and  $\text{Cu}_{rr}$   $d_{x^2-y^2}$  character and occupation numbers of nearly 1. The overall spin multiplicity is doublet, with the  $\text{Cu}_r$  and  $\text{Cu}_{rr}$   $3d$  electrons coupled antiferromagnetically.

Now, from this geometrical configuration we shift the  $\text{O}_b^l$  and  $\text{O}_b^c$  nuclei back to the high-symmetry, undistorted arrangement in steps of 1% of the Cu–O bond length. The orbitals from the previous step are used each time as input orbitals [14]. For the undistorted geometry the calculation converges to a state where the doped hole is mainly localized on the bridging  $\text{O}_b^l$  oxygen. Details regarding the composition and the occupation of the relevant orbitals are given in Table I. It was found that the energy of this  $\text{O}_b^l$ -hole state in the undistorted geometry is 320 meV higher than for the ZR like state in the configuration where the Cu– $\text{O}_b^l$  and Cu– $\text{O}_b^c$  bonds are 6% shorter. In agreement with the results from the previous section, between these two configurations a transfer of about one third of an electron/hole occurs from the  $\text{O}_b^l$   $p_y$  to the  $\text{O}_a^l$   $p_x$ ,  $\text{O}_b^c$   $p_y$ , and  $\text{Cu}_l$   $d_{x^2-y^2}$  orbitals, see Table I. The total cluster energy is plotted for different positions of the  $\text{O}_b^l$  and  $\text{O}_b^c$  oxygens in the left part of Fig.4.

For systems with competing valence configurations like our hole-doped cluster, different sets of input orbitals can lead to different solutions. We performed calculations where we forced the localization of the doped hole on the central  $\text{O}_b^c$   $p_y$  orbital, by adding some extra positive charge within our point charge embedding. Using

TABLE I: Contributions of various oxygen  $2p$  and metal  $3d$  atomic orbitals to the relevant Cu–O bonding (B) and antibonding (AB) active (natural) orbitals [13]. In each case, the other three active orbitals have essentially Cu  $d_{x^2-y^2}$  character and occupations of nearly 1. Coefficients smaller than 0.10 are not shown. Natural-orbital occupation numbers and Mulliken populations (MPs) are also given.  $O_b$  are bridging oxygens along the CuO chain, the  $O_a$  ions form parallel, adjacent in-plane O chains, see Fig.3(b).

State <sup>a</sup> :	$O_b^l$ -hole, undist. cluster			Cu <sub>l</sub> O <sub>4</sub> ZR, dist. Cu <sub>l</sub> –O <sub>b</sub> bonds <sup>b</sup>			$O_b^c$ -hole, undist. cluster		
	B	AB	MPs	B	AB	MPs	B	AB	MPs
$O_b^l p_y$	–	0.25	1.74	–	–	1.83	–	–	1.84
$O_a^l p_x$ (x2)	∓0.13	±0.26	1.70	–	–	1.83	–	–	1.85
Cu <sub>ll</sub> $d_{x^2-y^2}$	0.62	0.72	1.09	–	–	1.16	–	–	1.16
$O_b^l p_y$	0.66	–0.64	<b>1.27</b>	0.38	0.42	<b>1.62</b>	–	0.27	1.77
Cu <sub>l</sub> $d_{x^2-y^2}$	–0.18	–0.24	1.15	–0.63	0.79	1.01	–0.62	0.72	1.08
$O_a^l p_x$ (x2)	–	∓0.11	1.80	±0.33	±0.36	<b>1.64</b>	±0.13	±0.26	1.71
$O_b^c p_y$	–	–	1.83	–0.38	–0.42	<b>1.62</b>	–0.66	–0.64	<b>1.27</b>
Cu <sub>r</sub> $d_{x^2-y^2}$	–	–	1.15	–	–	1.15	0.18	–0.25	1.15
$O_a^r p_x$ (x2)	–	–	1.85	–	–	1.83	–	∓0.11	1.80
$O_b^r p_y$	–	–	1.84	–	–	1.84	–	–	1.83
Occ. No.	1.73	1.28		1.87	0.13		1.72	0.28	

<sup>a</sup> The fact that the doped holes have the largest weight on O  $p_x/p_y$  orbitals pointing to the Cu sites was also found in previous *ab initio* wave-function-based calculations [15, 16, 17]. Tendencies towards localization and broken-symmetry solutions were discussed in [16].

<sup>b</sup> The chain Cu<sub>l</sub>–O<sub>b</sub> bonds are 6% shorter.

this output as a new set of starting orbitals for CASSCF calculations with the initial embedding and no distortions, we were able to obtain a solution with a dominant contribution from the ...–Cu<sub>l</sub>  $d_{x^2-y^2}^1$ –O<sub>b</sub><sup>c</sup>  $p_y^1$ –Cu<sub>r</sub>  $d_{x^2-y^2}^1$ –... configuration. The energy of this state is 350 meV above the minimum corresponding to the ZR state on the distorted Cu<sub>l</sub>O<sub>4</sub> plaquette (see Fig.4). For the  $O_b^l$ -hole state, the Cu<sub>r</sub>  $d_{x^2-y^2}^1$ –Cu<sub>rr</sub>  $d_{x^2-y^2}^1$  AFM interactions are not perturbed by the presence of the oxygen hole and its relative energy is somewhat lower, 320 meV. The fact that the solution with the doped hole mainly localized on the  $O_b^c$  ligand is less accessible can be understood on the basis of this energy difference between the two  $O_b$ -hole states. Regarding the data in Table I and Fig.4 we also note that the  $O_b^c$ -hole doublet wave-function calculated for the undistorted geometry misses full  $D_{2h}$  symmetry. Attempts to converge to a fully symmetric wave-function were unsuccessful.

The structural configuration with 6% shorter chain Cu<sub>l</sub>–O bonds is symmetry equivalent to the situation where the chain Cu<sub>r</sub>–O bonds are 6% shorter. These two distorted configurations represent the minima of a one-dimensional double-well potential. From one minimum to the other, the sum of the Mulliken populations of the  $O_b$   $p_y$ ,  $O_a$   $p_x$ , and Cu  $d_{x^2-y^2}$  orbitals on each of the Cu<sub>l</sub>O<sub>4</sub> and Cu<sub>r</sub>O<sub>4</sub> plaquettes changes by about 0.7  $e$ . The total Mulliken electronic charge on each of these plaquettes changes between the two minima by about 0.5  $e$  (not shown in Table I) [18]. It is well known that the MPs are basis set dependent. Still, variations in the charge population of a whole CuO<sub>4</sub> plaquette (or CuO<sub>6</sub> octahe-

dron) is a reliable quantitative indicator. An illustrative result is also the variation of the total Mulliken electronic charge for the Cu<sub>l</sub>O<sub>6</sub> and Cu<sub>ll</sub>O<sub>6</sub> octahedra when going from the state with a Cu<sub>ll</sub>  $d_{x^2-y^2}^1$ –O<sub>b</sub><sup>l</sup>  $p_y^1$ –Cu<sub>l</sub>  $d_{x^2-y^2}^1$  leading configuration to the valence structure where the hole is mainly on the  $O_b^r$  oxygen. This value is 0.95  $e$ . About the same amount of charge, one hole/electron, should be transferred along the chain between “traveling” next nearest neighbor ZR singlets.

As mentioned in the previous section, we performed extra calculations on a 1-hole, 2-octahedra cluster. The doped hole is confined to a smaller region in space in this situation. In addition, charge relaxation effects within the neighboring chain octahedra can not be accounted for. Therefore, the CuO<sub>4</sub>–CuO<sub>4</sub> CT is weaker when distorting the CuO bonds, about 0.3  $e$ . For this smaller cluster it is possible however to use a more flexible active space, including all O  $2p$  and Cu  $3d$  orbitals. This corresponds to distributing 3 holes over 43 orbitals. With such an active space we found a CuO<sub>4</sub>–CuO<sub>4</sub> CT of 0.4  $e$  for the half-breathing distortions.

The results reported here are quite remarkable. They show that within a 1-doped-hole cluster including several CuO<sub>6</sub> octahedra, complex electron correlations give rise to quasi-localized O  $2p$  hole states and strong charge inhomogeneity. Several competing O-hole valence configurations were identified. The near-degeneracy between different hole configurations and the electron–lattice interactions cause strongly anharmonic, pseudo JT effects and facilitate the hopping of the charge carriers. Starting from a minimum-energy geometry where shorter “chain”

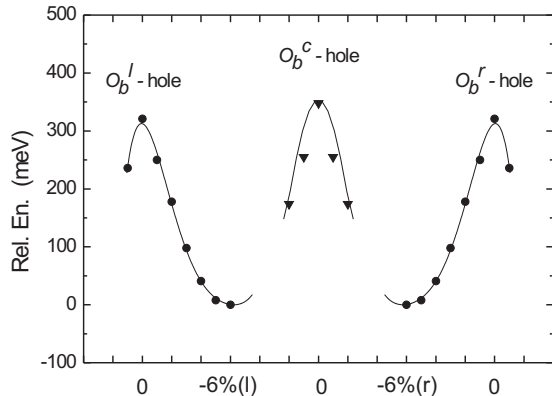


FIG. 4: Quasi-localized O-hole states on a 1-doped-hole, 4-octahedra linear cluster, see text. The energy maxima correspond to states with dominant  $O_b$ -hole character in the undistorted structure. The two minima are related to ZR like states where the Cu– $O_b$  distances on the  $Cu_lO_4$  plaquette (the left hand minimum) or the Cu– $O_b$  distances on the  $Cu_rO_4$  plaquette (the right hand minimum) are 6% shorter. From each minimum-energy structural configuration, the two  $O_b$  ligands are shifted back to the undistorted geometry in steps of 1% of the high-symmetry Cu–O bond length. The energies of these states are shown with black dots. The lines are a guide for the eye. The last point on each of these curves corresponds to a configuration where the Cu– $O_b$  distances on the  $Cu_lO_4/Cu_rO_4$  plaquette are shorter, by 1%. Other calculations were carried out for the case where the Cu– $O_b$  bonds on the  $Cu_lO_4$  and  $Cu_rO_4$  plaquettes are gradually shortened starting from the undistorted structure and using the orbitals of the  $O_b^c$ -hole state as starting orbitals. Due to convergence problems, only few points could be obtained. These points are shown as black triangles.

Cu–O bonds on a  $CuO_4$  plaquette give rise to a quasi-localized ZR like state, a half-breathing motion of the chain oxygens with a phase difference of  $\pi$  between adjacent plaquettes (see Fig.3(b)) leads to a  $CuO_4$ – $CuO_4$  charge transfer of about  $0.5e$  over an energy barrier of 350 meV (175 meV per chain oxygen). The minima of the one-dimensional double-well imply in-line O-atom displacements about the middle positions with amplitudes of only 0.11 Å ( $\pm 6\%$  of the Cu–O bond length). Although we did not investigate the effect of further Cu– $O_b$  distortions, it seems that a whole electron charge moves along the chain when a ...– $CuO_4$ –... [19] ZR like singlet is “transferred” to a next nearest neighbor plaquette.

It is possible that at about 1/6-doping an ordered arrangement of hole-free and 1/3-doped stripes is formed within the CuO plane [20]. Under this assumption our 1-hole, 4-octahedra cluster is related to the unit cell of the charge-ordered 1/3-doped stripe shown in Fig.3(a) (such a “unit cell” actually contains only three in-line octahedra). We speculate then that longer range hole–hole Coulomb interactions associated with cooperative, corre-

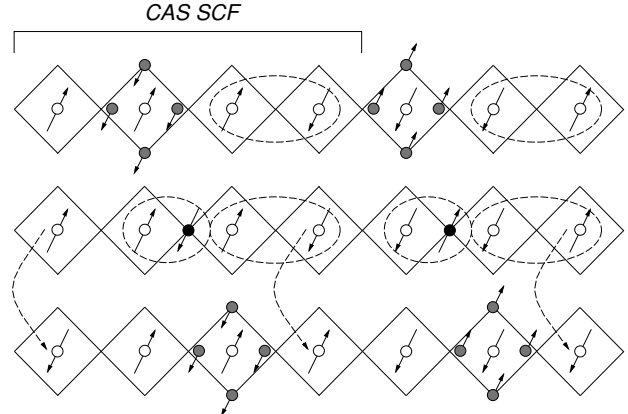


FIG. 5: Possible representation of the traveling charge-density/spin-density wave along a 1/3-doped  $CuO_4$ – $CuO_4$ –... chain. The O  $2p$  holes are shown with black or gray circles. For each sequence, the spins on the first four plaquettes display schematically [19] the CAS SCF results. The ellipses indicate spin-singlet couplings. Dashed arrows indicate a “spin-flip” process.

lated oxygen-atom displacements like those described in the previous paragraph along a chain of several  $Cu_lO_4$ – $CuO_4$ – $O_b^c$ – $Cu_rO_4$ – $O_b^r$  units should lower the energy barrier corresponding to the inter-site hole hopping and make possible an ordered, collective motion of the doped holes. Under the assumption of an alternating 1/3-doped/hole-free stripe configuration, our results seem to support thus a vibronic mechanism like proposed by Goodenough [1, 2] for the superconductivity in cuprates. It still needs to be investigated whether (and why) nearest neighbor 1-hole correlation bags would “cluster” along the chain to form a (traveling) CDW with spin-paired 2-hole, 4-Cu units separated by two antiferromagnetically-coupled Cu  $d^9$  ions as suggested in Ref. [2] (see Fig.1(a)). The longer range interactions responsible for the formation of such paired oxygen holes should be however weaker than those causing the local JT/CT effects we illustrate in Fig.4 and Table I. They probably merely modify the amplitudes of the O-atom displacements that determine the double-well potential. It should be pointed out at this stage that the CAS SCF results suggest that nearest neighbor oxygen holes have already antiparallel spins, see Fig.5.

Obviously, reliable estimates for the strength and the effects of the longer range couplings, intra- and inter-chain, are required for quantitative predictions. We note that in this model the effect of the inter-chain Coulomb interactions should be stronger for CuO multilayer structures like in the mercury compounds and might contribute to a higher  $T_c$ . The critical temperature  $T_c$  should be related to thermal fluctuations that disrupt the phase coherence among the kind of O-atom displacements described above. At temperatures well above  $T_c$  the striped arrangement is probably destroyed. For a certain temperature interval above  $T_c$ , the transition from

a charge-inhomogeneous phase with parallel chains (or fragments of chains) of 1-hole, 3-octahedra units but “uncorrelated” bond-length fluctuations to a totally disordered charge configuration could provide an explanation for the  $(\pi, \pi) - (\pi, 0)$  transfer of spectral weight in the angle-resolved photoemission spectroscopy (ARPES) data [22].

Our  $[\text{Cu}_4\text{O}_{21}]$  linear cluster seems to be a reasonable choice for studying local correlations for a 1/3-doped chain of octahedra. The quasi-localized character of the oxygen hole (see Table I) justifies such a material model. This cluster model would probably be inappropriate for the 1/2-doped chain (or stripe) in  $\text{La}_{1.48}\text{Nd}_{0.40}\text{Sr}_{0.12}\text{CuO}_4$  [24], where the doped-hole orbitals have much larger overlap. Also, although the CASSCF method can not yield highly accurate energies, such an approach is sufficient for an accurate description of the electron distribution provided the proper active space is chosen. The near-degeneracy and CT effects illustrated by our CASSCF results should be then a genuine characteristic of the  $\text{CuO}_4\text{-CuO}_4\text{-...}$  chain. On the other hand, the CASSCF data normally gives a rather qualitative (or semi-quantitative) description for potential-energy landscapes like that associated with the O-atom half-breathing displacements. A more elaborate treatment, *e.g.* multi-reference configuration-interaction or multiconfiguration perturbation theory [6], is needed for calculating accurate potential curves and surfaces. Such calculations will be documented in an upcoming publication.

A matter of concern with our calculations may be the fact that we used experimental structural data. It would be desirable to start, for example, from a fully optimized structural configuration of the undoped system. For such an optimized geometry, the in-plane Cu-Cu distance would be of particular interest. It is known that the *ab initio* periodic Hartree-Fock (HF) calculations in the linear-combination of atomic orbitals (LCAO) formulation slightly overestimate the lattice parameters in transition metal oxides, for example by 2% in MnO and NiO [25] and almost 4% in  $\text{Cu}_2\text{O}$  [26]. To reduce these deviations, post-HF techniques are needed [27]. Nevertheless, structure optimizations for complex periodic systems like  $\text{La}_2\text{CuO}_4$  at a correlated, post-HF level are not possible yet. Intuitively, we expect that for slightly larger Cu-Cu distances in our cluster the doped hole is somewhat more localized on the distorted  $\text{CuO}_4$  plaquette (see Table I). In this case the half-breathing O-atom vibrations should imply more CT between adjacent plaquettes but over a higher energy barrier.

#### IV. CONCLUSIONS

We study local electron correlation effects for hole-doped CuO clusters including several  $\text{CuO}_6$  octahedra. We use the structural data reported for the tetragonal lattice of  $\text{La}_{1.85}\text{Sr}_{0.15}\text{CuO}_4$ . Results of *ab initio* MCSCF

calculations on a 1-hole, 4-octahedra linear cluster indicate a double-well potential for half-breathing O-atom displacements along the O-Cu-O-Cu-O row. The Cu-O bond-length fluctuations are coupled with large intersite charge transfer effects. For distortions of  $\pm 6\%$  of the Cu-O bond length, charge fluctuations of about  $0.5e$  are observed between nearest neighbor  $\text{CuO}_4$  plaquettes. It seems also that a whole electron charge would move along the chain when a  $\text{...-CuO}_4\text{-...}$  ZR like singlet is transferred to a next nearest neighbor plaquette.

For a 1/6-doped CuO plane we adopt the hypothesis of charge segregation [20] into alternating 1/3-doped and hole-free Cu-O-... stripes of Goodenough *et al.* [1, 2]. Under the charge segregation hypothesis, our findings seem to support the vibronic mechanism and the traveling charge-density/spin-density wave (CDW/SDW) model of Goodenough for the high- $T_c$  superconductivity in cuprates. In this scenario the superconducting state would imply long range “correlation” (or phase coherence) among the type of O-atom displacements shown in Fig.3(b). We arrive in the end to the kind of picture proposed by Egami *et al.* [21]: electron correlation — according to our calculations, the near-degeneracy between the quasi-localized ZR like state on a  $\text{CuO}_4$  plaquette and a state whose leading configuration is of the form  $\text{Cu } d^9\text{-O } p^5\text{-Cu } d^9$  plus the longer range hole-hole Coulomb repulsion — is the engine, while the driver is the lattice vibration.

Work combining results of first principles MCSCF calculations on small clusters and results of calculations for a Hubbard type model Hamiltonian on extended  $\text{CuO}_4\text{-CuO}_4\text{-...}$  chains is in progress. It is hoped that such investigations will enable reasonable estimates of the longer range interactions and other (quantitative) predictions. In a recent study combining the two approaches we were able to give a rather realistic description of the phase transition in the mixed-valence  $\text{NaV}_2\text{O}_5$  compound [29]. “Correlated” calculations for a bi-dimensional Cu-O structure to investigate the charge segregation scenario in the CuO plane at 1/6-doping are unfeasible at this moment.

The JT/CT effects illustrated by our *ab initio* results are much too robust to be taken just as an artifact of our finite clusters or/and of other approximations. We believe that these results define a few basic requirements that a model Hamiltonian approach should meet for realistic predictions in the optimally doped and under-doped copper oxide compounds.

#### V. ACKNOWLEDGEMENTS

We thank O. K. Andersen and O. Jepsen for encouraging this study and A. T. Filip, O. Gunnarsson, and G. Stollhoff for fruitful discussions. L. H. acknowledges financial support from the Alexander von Humboldt Foundation.

- 
- [1] J. B. Goodenough, *Europhys. Lett.* **57**, 550 (2002).
- [2] J. B. Goodenough, *J. Phys.: Condens. Matter* **15**, R257 (2003).
- [3] J. Q. Yan, J. S. Zhou and J. B. Goodenough, *New Journal of Physics* **6**, 143 (2004).
- [4] F. C. Zhang and T. M. Rice, *Phys. Rev. B* **37**, 3759 (1988).
- [5] R. J. Cava, A. Santoro, D. W. Johnson, and W. W. Rhodes, *Phys. Rev. B* **35**, 6716 (1987).
- [6] For a monograph, see T. Helgaker, P. Jørgensen, and J. Olsen, *Molecular Electronic-Structure Theory* (Wiley, Chichester, 2000).
- [7] S. Huzinaga, L. Seijo, Z. Barandiarán, and M. Klobukowski, *J. Chem. Phys.* **86**, 2132 (1987); L. Seijo, Z. Barandiarán and S. Huzinaga, *ibid.* **91**, 7011 (1989).
- [8] P.-O. Widmark, P.-Å. Malmqvist, and B. O. Roos, *Theor. Chim. Acta* **77**, 291 (1990).
- [9] MOLCAS 6, Department of Theoretical Chemistry, University of Lund, Sweden.
- [10] The calculations were performed with  $C_h$  symmetry restrictions, with the  $xy$  plane as a mirror plane.
- [11] P. S. Bagus, R. Broer, C. de Graaf, W. C. Nieuwpoort, *J. Elect. Spectrosc. Related Phen.* **98-99**, 303 (1999).
- [12] R. Pou-Amérigo, M. Merchán, I. Nebot-Gil, P.-O. Widmark, and B. O. Roos, *Theor. Chim. Acta* **92**, 149 (1995).
- [13] The natural orbitals are obtained such as to diagonalize the one-electron density matrix.
- [14] A set of input orbitals must be provided for the CAS SCF calculation. These input orbitals can either be from a Hartree-Fock closed-shell ( $\text{Cu } d^{10} \text{O } p^6$ ) calculation or from a previous CAS SCF calculation on the same system.
- [15] C.-J. Mei and G. Stollhoff, *Phys. Rev. B* **43**, 3065 (1991); G. Stollhoff, *Phys. Rev. B* **58**, 9826 (1998).
- [16] R. L. Martin, *J. Chem. Phys.* **98**, 8691 (1993); R. L. Martin, *Phys. Rev. B* **53**, 15501 (1996).
- [17] C. J. Calzado, J. F. Sanz, and J. P. Malrieu, *J. Chem. Phys.* **112**, 5158 (2000).
- [18] The Mulliken electronic charges of the apical ligands remain nearly constant.
- [19] The O  $2p$  hole also has some weight on farther anions, see Table I.
- [20] There is much experimental data that suggest the formation of such stripes, see for example the discussions in [1, 2], [21] and references therein.
- [21] T. Egami, Y. Petrov, and D. Louca, *J. Supercond.: Incorpor. Novel Magn.* **13**, 709 (2000).
- [22] See for example [2], [23], and references therein.
- [23] A. Damascelli, Z. Hussain, and Z.-X. Shen, *Rev. Mod. Phys.* **75**, 473 (2003).
- [24] J. M. Tranquada, B. J. Sternlieb, J. D. Axe, Y. Nakamura, and S. Uchida, *Nature* **375**, 561 (1995).
- [25] M. D. Towler, N. L. Allan, N. M. Harrison, V. R. Saunders, W. C. Mackrodt, and E. Aprá, *Phys. Rev. B* **50**, 5041 (1994).
- [26] E. Ruiz, S. Alvarez, P. Alemany, and R. A. Evarestov, *Phys. Rev. B* **56**, 7189 (1997).
- [27] Algorithms able to treat electron correlation explicitly in periodic systems are being developed, see for example [15, 28].
- [28] A. Shukla, M. Dolg, P. Fulde, and H. Stoll, *Phys. Rev. B* **60**, 5211 (1999); P. Y. Ayala, K. N. Kudin, and G. E. Scuseria, *J. Chem. Phys.* **115**, 9698 (2001); S. Hirata, R. Podaszwa, M. Tobita, and R. J. Bartlett, *J. Chem. Phys.* **120**, 2581 (2004).
- [29] L. Hozoi, S. Nishimoto, and A. Yamasaki, cond-mat/0501757 (unpublished); L. Hozoi, C. Presura, C. de Graaf, and R. Broer, *Phys. Rev. B* **67**, 035117 (2003).